

Self-Energized Wireless Pressure Sensor Using Energy Extraction from Injection Mold Pressure Differential

Charles B. Theurer

Department of Mechanical and Industrial Engineering
University of Massachusetts Amherst
Amherst, MA 01003
Email: Ctheurer@ecs.umass.edu

David Kazmer

Department of Plastics Engineering
University of Massachusetts Lowell
Lowell, MA 01854
Email: David_Kazmer@uml.edu

Li Zhang

Department of Mechanical and Industrial Engineering
University of Massachusetts Amherst
Amherst, MA 01003
Email: Lizhang@ecs.umass.edu

Robert X. Gao, Senior Member, IEEE

Department of Mechanical and Industrial Engineering
University of Massachusetts Amherst
Amherst, MA 01003
Email: Gao@ecs.umass.edu

Abstract

With the prolific use of sensors for manufacturing process monitoring and the growing demand for system integration, the issue of packaging and installation has assumed an increasingly central role. Cable-based sensors, while still the common form on the factory floor, face various constraints in real-world machine environments. Battery-based operation, although compact and eliminating the cable attachment, has the ultimate drawback of periodic battery replacement due to wear-and-tear. Thus, it would be ideal if energy can be “extracted” from the manufacturing process being monitored itself to enable “self-energized” sensing.

This paper presents the design of a self-energized pressure sensor that extracts energy from the pressure differential of the polymer melt during the injection molding process. A piezoelectric element is used as the energy converter to convert the high melt pressure into proportional electrical charges, which in turn, actuate an ultrasound signal through a miniature energy switch. Based on predetermined energy threshold values, the actuator generates a train of ultrasound pulses, which represent the continuous melt pressure in a digitized form. The ultrasound pulses propagate wirelessly through the mold steel and are detected by a remotely located signal receiver. Through multiplication of the number of pulses with the energy threshold values, the polymer melt pressure profile is reconstructed.

To enable a self-energized sensor design, an analytical study has been conducted to establish a quantitative relationship between the polymer melt pressure and the energy that can be extracted through the use of a piezoelectric converter. Two models have been developed and compared to an energy extraction prototype. First, a linear model examining the energy conversion mechanism due to interactions between the mechanical strain and the electric

field developed within the piezoelectric device is established. Second, using a coupled-field analysis, a numerical model is developed to evaluate the electromechanical properties dependent upon the geometric effects of the piezoelectric converter. Finally, the two models are compared to a functional prototype design to evaluate the relevance of the assumptions and accuracy of the models developed.

The presented design enables a new generation of self-energized sensors that can be employed for the condition monitoring of a wide range of high-energy manufacturing processes.

Keywords

Pressure Sensor, Wireless Sensor, Piezoelectric Energy Extraction, Acoustic Telemetry, Threshold Sensor

INTRODUCTION

It has been shown that direct cavity pressure and temperature measurement, more than any indirect method, is related to final part quality produced by the injection molding process [1-3]. For this reason the development of a low cost, reliable cavity pressure measurement system has been the subject of this research. A typical cavity pressure sensor in an injection mold consists of a measurement diaphragm connected by a capillary tube to another measurement diaphragm that is remote to the process where the information is translated from a mechanical signal to an electrical signal. Because of the complexity of most injection molds, the cost to install such a device can be on the order of the cost of the sensor itself. The majority of the installation cost is associated with cabling or providing a pathway for the information to travel from the sensor to the process controller. These problems are not new to industry and have been fueling the development of wireless sensor technology for many years. Injection molding, however, presents special problems associated with the development of a wireless

sensor system [4]. The presence of a steel cavity completely surrounding the sensor makes it nearly impossible to effectively communicate a process signal using traditional wireless means. In a traditional wireless sensor, the power source for the sensor must be contained in the sensor itself. The power source for a long life sensor can be very large in comparison to the size of the sensing equipment. However, such a design strategy leads to an undesirably large sensor. As such, it has been proposed that the pressure differential associated with the filling and packing of an injection mold might be used to generate electricity using a piezoelectric element [5].

The proposed self energized wireless sensor would be installed in the cavity of the injection mold, extract energy from the injection pressure, and send the pressure information in the form of a train of ultrasonic pulses through the mold steel to an acoustic receiver located outside the mold. Such a wireless pressure sensor makes it economically possible to have multiple sensors per cavity or a sensor in each cavity of a multi-cavity mold (Figure 1).

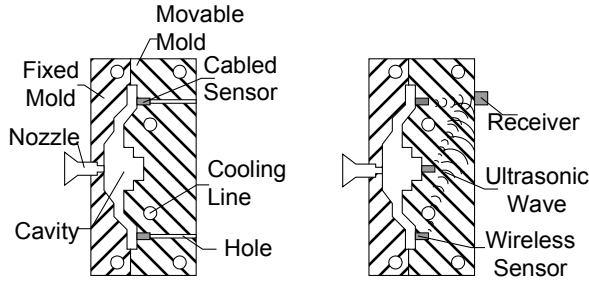


Figure 1. Existing cabled cavity pressure sensor (left) and remote cavity pressure sensor (right)

The piezoelectric method of energy extraction is the subject of this paper. Two models are developed and compared to an energy extraction prototype. First, a static analytical model is developed, similar to models provided by many piezoelectric material manufacturers [6-8]. Second, a finite element model is developed using a coupled field analysis method to determine the electrical and mechanical transient behavior of a single ceramic element. Finally, a functional prototype is developed to validate the accuracy of the two models.

MODEL DEVELOPMENT

When a stress is applied to a piezoelectric element it generates a charge. This charge is associated with the deformation of the highly polarized molecules in the crystal structure. If electrodes are placed on opposite sides of the crystal, the charge can be collected and used. The energy stored in the element is stored in two forms: 1) electrically in the form of an electric field and, 2) mechanically in the form of strain. The interaction between the strain and the electric field is the subject of the first model presented.

The electromechanical behavior of a piezoelectric element is also heavily dependant on the geometry of that element. As piezoelectric devices are increasingly used, the manufacturable geometry of these devices becomes more complex. In order to model the electromechanical properties of geometrically complex piezoelectric elements, finite element models are also developed and evaluated.

Linear Model

Constitutive Equations

The relationship between the electrical and mechanical behavior of a piezoelectric material in general can be described using two piezoelectric constants; a piezoelectric charge constant, equations (1) and (2), and a piezoelectric voltage constant, equations (3) and (4).

$$d = \frac{\text{dielectric displacement developed}}{\text{applied mechanical stress}} = \frac{D}{T} \quad (1)$$

$$d = \frac{\text{strain developed}}{\text{applied electric field}} = \frac{S}{E} \quad (2)$$

$$g = \frac{\text{electric field developed}}{\text{applied mechanical stress}} = \frac{E}{T} \quad (3)$$

$$g = \frac{\text{strain developed}}{\text{applied dielectric displacement}} = \frac{S}{D} \quad (4)$$

One of the constitutive equations associated with the charge constant relates stress and electric field to the strain [9]

$$S = s^E \cdot T + d \cdot E \quad (5)$$

where s^E is the compliance of the material in a constant electric field (i.e. electrically shorted). It is interesting to note that the first term of this equation is essentially Hook's law for elastic materials while the second term indicates the strain associated with the electric charge. The other constitutive equation associated with the charge constant relates stress and electric field to the electric displacement

$$D = d \cdot T + \epsilon^T \cdot E \quad (6)$$

where ϵ^T is the permittivity of the material where the stress is uniform in the material.

The constitutive equations associated with the voltage constant are presented in a similar manner [6]

$$E = -g \cdot T + \frac{D}{\epsilon^T} \quad (7)$$

$$S = s^D \cdot T + g \cdot D \quad (8)$$

where s^D is the constant electric displacement compliance (i.e. electrically open). Substituting equation (7) into equation (6) reveals the relationship between d and g as

$$d = \epsilon^T \cdot g \quad (9)$$

Energy balance

If the system is electrically shorted, the electric field is uniform and no electrical energy is stored in the system. However if the system is electrically open, energy is stored in the material in two forms; electrical and mechanical. The principal of the conservation of energy and the assumption that energy is not lost to friction or electrical resistance leads to the following equation:

$$[W_D] = [W_m] + [W_e] \quad (10)$$

where W_D is the work due to displacement or the total energy imparted to the system, W_m is the total mechanical energy stored in the system, and W_e is the total electrical energy stored in the system. If the assumption is made that the material behaves elastically, then W_D can be expressed in another way [6],

$$W_D = \frac{\text{Vol}}{2} \cdot s^D \cdot T^2 \quad (11)$$

where Vol is the volume of the material. W_m can be expressed as

$$W_M = \frac{\text{Vol}}{2} \cdot s^E \cdot T^2 \quad (12)$$

and substituting equations (11) and (12) into (10) yields

$$W_E = \frac{\text{Vol}}{2} (s^D - s^E) T^2 \quad (13)$$

At this point it is appropriate to introduce a derived material constant that relates the total energy converted to the total energy density of the system. If we define the piezoelectric coupling factor k as

$$k^2 = \frac{\left[\begin{array}{c} \text{total stored energy} \\ \text{density for freely} \\ \text{deformed PXE body} \end{array} \right] - \left[\begin{array}{c} \text{electrical energy} \\ \text{density for} \\ \text{constrained PXE body} \end{array} \right]}{\left[\begin{array}{c} \text{total stored energy} \\ \text{density for freely} \\ \text{deformed PXE body} \end{array} \right]} = \frac{\left[\begin{array}{c} \text{stored converted} \\ \text{mechanical} \\ \text{energy density} \end{array} \right]}{\left[\begin{array}{c} \text{total stored} \\ \text{energy density} \end{array} \right]} \quad (14)$$

then assuming the volume doesn't change when a pressure is applied to the element the piezoelectric coupling factor becomes

$$k^2 = - \frac{(s^D - s^E)}{s^E} \quad (15)$$

Geometry considered

A piezoelectric ring, such as the one shown in Figure 2, when loaded parallel to the axis of symmetry (the 3 direction), is in a state of approximately constant stress through the thickness. If this ring was also polarized in the axial direction, the above constitutive model can be applied.

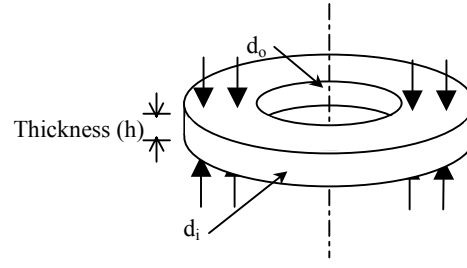


Figure 2. A piezoelectric ring loaded along the top and bottom surfaces and polarized along the axis of symmetry

In the application to a mold cavity pressure sensor, the above crystal would have a cap separating it from the molten plastic. This cap decouples the area of the ring and the force acting on the ring. The force placed on the ring in compression is

$$F = \pi \frac{d_o^2}{4} \text{press} \quad (16)$$

where press is the pressure acting on the cap surface. Stress in the piezoelectric ring can then be calculated by

$$T = \frac{F}{A_{cr}} \quad (17)$$

where A_{cr} is the crystal area

$$A_{cr} = (d_o^2 - d_i^2) \pi / 4 \quad (18)$$

From equations (13), (16), (17), and (18) we can now calculate the energy associated with applying a given pressure to the crystal in Figure 1.

$$W_e = \frac{d_{33}^2 \cdot h \cdot d_o^4 \cdot \pi \cdot s_{33}^D \cdot \text{press}^2}{8(d_o^2 - d_i^2) \cdot \epsilon_{33}^T \cdot s_{33}^E} \quad (19)$$

The voltage across the electrodes in an open circuit is readily calculated using the definition of the voltage constant in equation 3

$$V = g_{33} \cdot \frac{d_o^2 \text{press}}{d_o^2 - d_i^2} \cdot h \quad (20)$$

Similarly the charge can be calculated using the definition of charge constant in equation 1

$$Q = \frac{d_{33} \cdot \pi \cdot d_o^2 \cdot \text{press}}{4} \quad (21)$$

Finally, the open and closed circuit displacements can be calculated from the definition of compliance

$$\Delta h_{\text{open}} = s^D \cdot h \cdot \frac{\text{press} \cdot d_o^2}{(d_o^2 - d_i^2)} \quad (22)$$

$$\Delta h_{\text{closed}} = s^E \cdot h \cdot \frac{\text{press} \cdot d_o^2}{(d_o^2 - d_i^2)} \quad (23)$$

where s^D and s^E are related to each other through the piezoelectric coupling coefficient defined in equation 14.

The linear nature of this model produces some weaknesses that should be noted. While the piezoelectric effect is captured in the above model, there are several transient and temperature effects that are not. The pyroelectric effect, defined by [10, 11] to be electric charge produce as a result of a temperature change, is not captured by the above model. The conversion of electrical and mechanical energy to heat through resistance and friction respectively are also ignored as well as the inertial effects associated with high strain rates.

FINITE ELEMENT MODEL

The complexity of the preceding linear model would suggest that the use of the finite element method with some simplifications might be of use when the geometry is anything but trivial. The finite element formulation used is essentially a compromise between the simplified static model and a more complex transient model. This finite element model uses a formulation similar to the static model but also incorporates Newton's second law and some material damping effects to give a transient approximation that ignores electrical losses and thermal effects. The models below attempt to closely follow the geometry and boundary conditions that are represented in Figure 3.

2D static model

A 2D axisymmetric static coupled field analysis of a simple piezoelectric ring (Figure 2) was developed in ANSYS using Plane-13 elements [12].

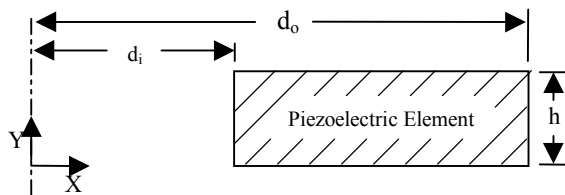


Figure 3. 2D axisymmetric representation of a piezoelectric ring

A convergence check was performed to determine an appropriate element size that results in acceptably accurate results in short solution time (Figure 4). It was determined that an element edge length of 0.2 mm corresponding to four elements through the thickness direction and a total solution time of less than 1 second satisfied this criteria for the 2D model.

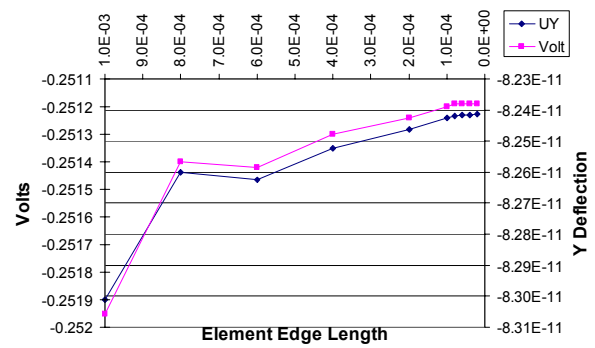


Figure 4. 2D axisymmetric model convergence check

3D Static Model

In order to check the validity of the 2D modeling assumptions, a 3D coupled field analysis was also developed and a convergence check was performed (Figure 5, 6).

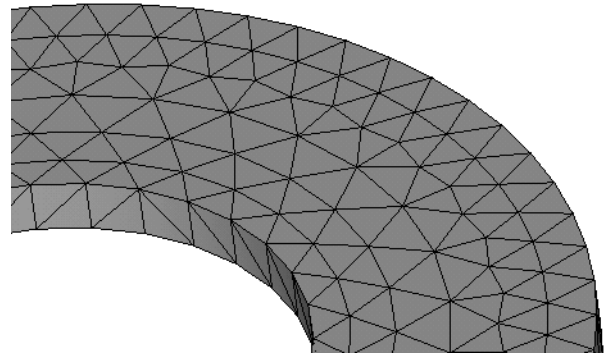


Figure 5. 3D mesh of a piezoelectric ring

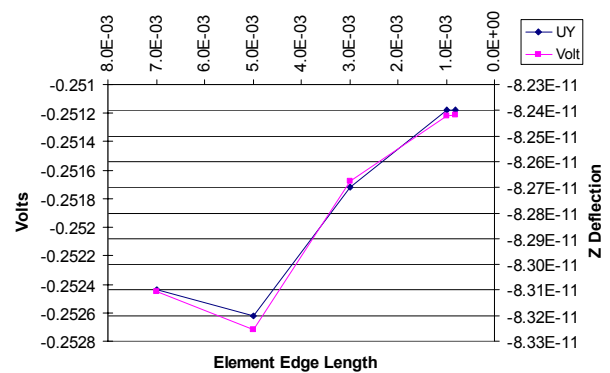


Figure 6. 3D model convergence check

2D-3D Model Comparison

Once the 2D and 3D models were developed, the static results for a given pressure load were compared. Because of the use of the coupled field analysis, both the voltage and displacement fields were compared. The results were in very good agreement; the voltage fields agreed within 0.01% (Figure 7), while the displacement results agreed

within 0.05% (Figure 8).

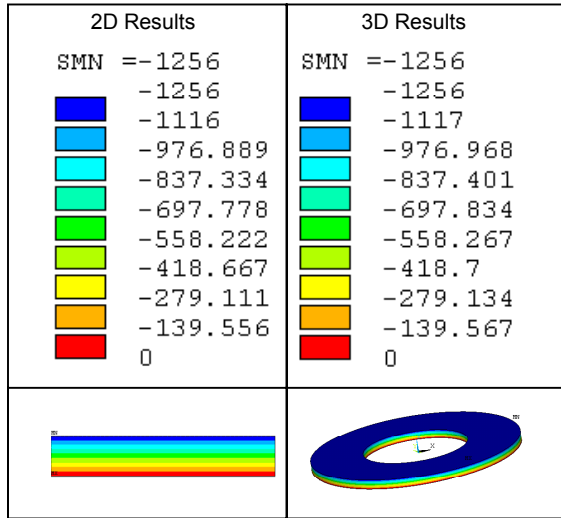


Figure 7. 2D and 3D voltage results agree within 0.01%

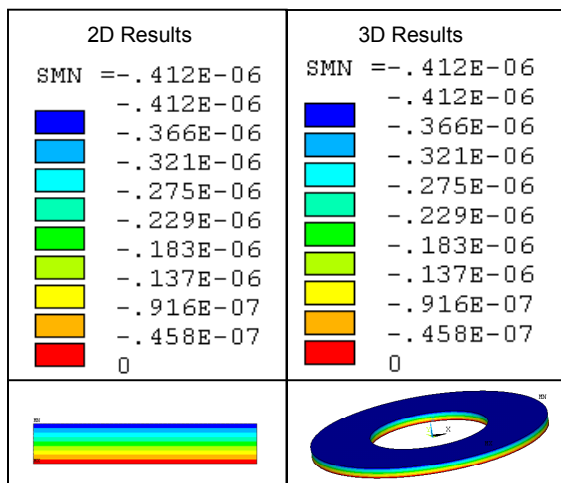


Figure 8. 2D and 3D displacement results agree within 0.05%

The agreement between the 2D and 3D models indicates that it is appropriate to use geometry and boundary conditions associated with the 2D axisymmetric model.

FE Transient Results

A transient analysis was performed in order to simulate the ramping of the pressure during an actual injection molding cycle. The pressure was ramped at 500Mpa/sec and is fairly representative of that occurring in the actual injection molding process. At some time during the injection process, the energy stored electrically in the piezoelectric crystal must be used. One scenario for this change in potential can be modeled by allowing the electric field to change freely in the element, simulating an open circuit, then applying a

boundary condition that forces the electric field on the top and bottom to be equal, simulating a short circuit (Figure 9).

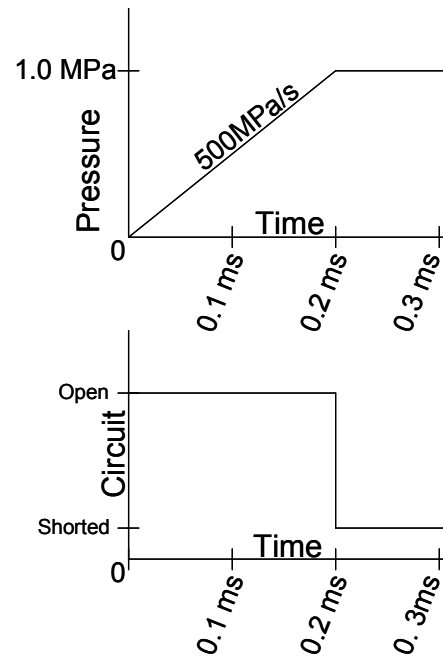


Figure 9. Pressure and electric field curves for the transient FE analysis

The resulting displacement and vibration of the piezoelectric ring is shown in Figure 10. As the pressure is applied the displacement increases linearly. The abrupt change in displacement is associated with the application of the electric field boundary condition indicated in Figure 9. Subsequently, some vibration is observed as the ring obtains another steady state. The results obtained from the above transient analysis indicate that the model does capture the piezoelectric effect as well as the inertial and damping effects of the material

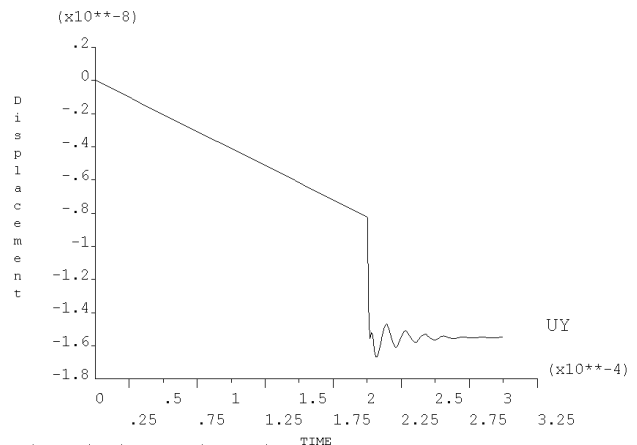


Figure 10. Pressure and electric field curves for the transient FE analysis

Linear Model Comparison

This change in the voltage of the material, associated with the change from s^D to s^E is in agreement with the linear model presented above. A comparison between the linear and the FE Model can now be performed.

Vendor supplied information, shown in Table 1, for the piezoelectric material lead zirconate-titanate PZT-4 was applied to both models.

Table 1. Properties applied to each of the models for the purposes of comparison

Description	PZT-4	Units
ρ	7500	kg/m ³
d_{31}	-1.23E-10	m/V
d_{33}	2.89E-10	m/V
d_{15}	4.96E-10	m/V
s_{11}^E	1.23E-11	m s ² /kg
s_{33}^E	1.55E-11	m s ² /kg
s_{12}^E	-4.05E-12	m s ² /kg
s_{13}^E	-5.31E-12	m s ² /kg
s_{44}^E	3.90E-11	m s ² /kg
s_{66}^E	NA	m s ² /kg
K'_{11}	1475	(unitless)
K'_{33}	1300	(unitless)
ϵ_0	8.85E-12	F/m

For a pressure of 50 MPa and an outside diameter and inside diameter of 10 mm and 5 mm respectively and a thickness of 1 mm the voltage results for the linear model and the FE model are 1673.3 V and 1675 V respectively. These results agree within approximately 0.1%

EXPERIMENTAL RESULTS

A ten disk prototype stack was created in order to evaluate the previous two models with respect to experimental results.

Experimental Setup

Ten piezoelectric rings were placed in a stack so that they were electrically in parallel (Figure 11). The stack was then placed in an apparatus that allowed a force to be applied along the axial direction. A load cell was placed under the stack in order to simultaneously measure the force acting on the stack and its electrical output (Figure 12).

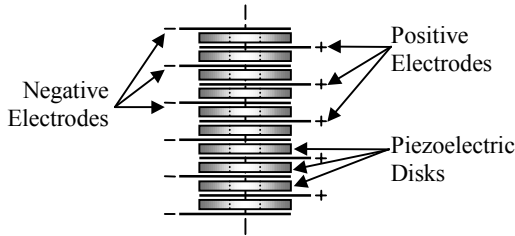


Figure 11. Schematic diagram of the prototype stack

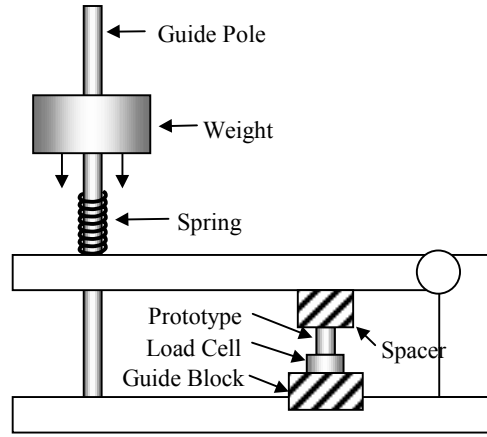


Figure 12. Schematic Diagram of Prototype loading apparatus

Two scenarios were then evaluated, in both cases force was applied to the stack; 1) the stack was connected to the measuring scope (10 M Ω), simulating as close as possible an electrically open circuit, and 2) the a resistor (99.4 k Ω) was connected between the electrodes of the stack (simulating an electrically closed circuit to ground).

Experimental Results

The loading and unloading of the piezoelectric stack spanned approximately 0.12 seconds. During this time current will be lost through the measuring device in scenario 1 and through both the scope and the parallel resistor in scenario 2. There is no correction for this effect in the linear model presented above. In order to compare the linear model to experimental results it is necessary to predict this voltage loss and include it in the model. The electrical nature of the piezoelectric stack is that of a capacitor. Equation 24 represents the voltage loss through the capacitor during a single time step Δt .

$$V_{i(\text{loss})} = V_{(i-1)} - (V_{(i-1)} \cdot e^{-\Delta t/(R \cdot C)}) \quad (24)$$

Where $V_{i \text{ loss}}$ is the voltage lost through the resistor R for the time step i, V_{i-1} is the predicted voltage for the previous time step, and C is the measured capacitance of the piezoelectric prototype stack. The predicted voltage can then be calculated by adding the voltage change predicted by the linear model to the voltage change predicted by equation 24 for each discrete time step in the loading cycle (Equation 25).

$$V_i = V_{i-1} + \Delta V_{i(\text{linear model})} + V_{i(\text{loss})} \quad (25)$$

The stress in piezoelectric elements was assumed to be constant in the axial direction and was approximated using the load-cell output. This stress, along with the measured voltage, and the voltage predicted by the linear model are represented in Figure 13 for scenario 1 and Figure 14 for scenario 2.

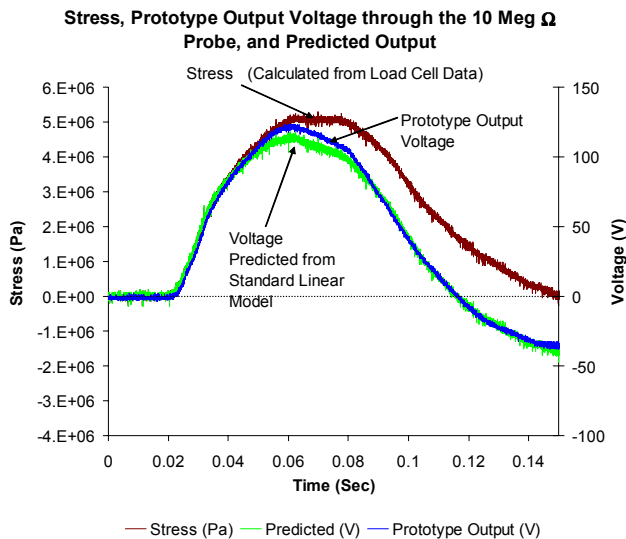


Figure 13. Stress in the piezoelectric elements, prototype output voltage, and predicted output voltage for scenario 1

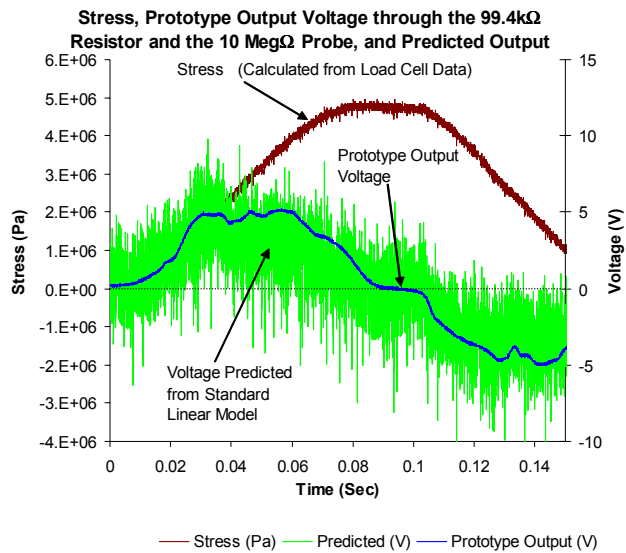


Figure 14. Stress in the piezoelectric elements, prototype output voltage, and predicted output voltage for scenario 2

As can be seen in both Figures 13 and 14, the measured voltage does not exactly track the stress in the material as the standard model would predict. The difference is due to the losses associated with the measurement of the signal in scenario 1 and with the current through the 99.4 kΩ resistor. As the voltage across the stack electrodes increases, current is lost through the probe in scenario 1 and through the parallel resistor in scenario 2 according to Equations 24 and 25

The large amount of high frequency noise associated with

the predicted voltage in Figure 14 is a result of the fact that the predicted voltage is based on the stress in the stack, as measured by the load cell. The load cell signal is comparatively noisy and results in a noisy predicted voltage. The rise in voltage between 0.13 and 0.15 seconds is a result of the fact that the voltage is negative and as a result the current in the resistor is reversed (Equation 24).

RESULTS AND DISCUSSION

A linear model of energy extraction from a piezoelectric element was derived from the governing constitutive equations. This model was compared to a finite element model and an experimental prototype. The linear model agrees with the finite element model within approximately 0.1%, while it agreed with the experimental results within approximately 5%. A comparison of the energy output of the linear model and the prototype can be seen in Table 2. The total amount of energy developed by the prototype stack agrees within about 10% of the predicted energy. Because the energy is extracted over a very short time duration (approximately 0.1 seconds) the average power output of the prototype stack is over 1.5 mW.

Table 2. Comparison of the total energy output of the linear model and the prototype

Experimental Values				
Energy (J)	Measured	Energy In Cap	0.1135 (mJ)	
		Energy through R	0.0424 (mJ)	
		Total Energy	0.1559 (mJ)	
		Average Power	1.5587 (mWatt)	
		Energy In Cap	0.1039 (mJ)	
	Predicted	Energy through R	0.0362 (mJ)	
		Total Energy	0.1401 (mJ)	
		Average Power	1.4011 (mWatt)	
		Max	Stress	5.295 (MPa)
			Pressure	3971.0 (MPa)

If the previous dataset were scaled such that the maximum pressure were representative of an actual injection molding cycle, in the same time, the predicted output power would be approximately 890 mW, as can be seen in Table 3.

Table 3. Energy comparison of experimental dataset scaled to match injection molding process characteristics

Scaled Experimental Values				
Energy (J)	Measured	Energy In Cap	72.96 (mJ)	
		Energy through R	27.27 (mJ)	
		Total Energy	100.23 (mJ)	
		Average Power	1002.26 (mWatt)	
		Energy In Cap	66.10 (mJ)	
	Predicted	Energy through R	22.94 (mJ)	
		Total Energy	89.05 (mJ)	
		Average Power	890.48 (mWatt)	
		Max	Stress	133.33 (MPa)
			Pressure	100.00 (Mpa)

Comparatively, a typical AAA alkaline battery is rated to produce approximately 3.75 mW continuously [13].

CONCLUSIONS

In conclusion, the two models developed compare favorably to the prototype. The linear model can be implemented in a circuit simulation program in order to provide a useful

tool in the integration of the energy extraction, pressure encoding, and acoustic signal generation sub-systems. The FEA model may provide a useful tool in the development of the more geometrically complex piezoelectric transmitter.

The predicted energy output is also significant in comparison to that of a typical alkaline battery; the prototype piezoelectric stack is predicted to produce approximately 250 times the power of a AAA alkaline battery during a typical molding cycle, which should prove sufficient to generate and transmit an acoustic signal that can be received outside the mold. Use of this energy to encode a pressure signal is discussed in more detail in [14]. The process by which this encoded electrical signal can be used to generate an encoded acoustic signal and be transmitted through the mold is the subject of [15].

ACKNOWLEDGEMENT

The authors gratefully acknowledge funding provided by the National Science Foundation under grant #DMI-9988757.

REFERENCES

- [1] I. A. Rawabdeh and P. F. Petersen, "In-Line Monitoring of Injection Molding Operations: A Literature Review," *Injection Molding Technology*, Vol. 3, pp. 47-53, 1999.
- [2] B. Watkins, "Five Myths about Sensing Mold Pressure," in *Sensors Magazine*, Vol. 14, 1997, pp. 73-78.
- [3] Federico Manero, W. I. Patterson, and Musa R. Kamal, "Cavity temperature profile measurement during injection moulding," presented at Annual Technical Conference - ANTEC, Conference Proceedings, 1997.
- [4] C. Theurer, L. Zhang, R. Gao, and D. Kazmer, "Acoustic telemetry in injection molding," presented at Process Monitoring And Control Division, Society of Plastics Engineers Annual Technical Conference, Dallas, TX, 2001.
- [5] C. Theurer, "Investigation of a Remote Pressure Sensor For Real Time Control Of An Injection Molding Machine," MS. project report, Dept. of Mechanical and Industrial Engineering, University of Massachusetts, Amherst, 2001.
- [6] J. W. Waanders, "Piezoelectric Ceramics Properties and Applications", Philips, Eindhoven, NL, 1991.
- [7] Morgan Electro Ceramics, "Piezoelectricity Tutorial," Vol. 2001.
- [8] Channel Industries, "Piezoelectric Ceramics Equations," 2001.
- [9] J. Van Randerat and R. E. Settrington, "Piezoelectric Ceramics", 2nd Ed. Mullard, London, UK, 1974.
- [10] Piezo Systems, "Introduction to Piezoelectricity," Piezo Systems Inc., 2001.
- [11] Won-kyu Moon and Ilene J. Busch-Vishniac, "Modeling of piezoelectric ceramic vibrators including thermal effects. Part I. Thermodynamic property considerations," *The Journal of the Acoustical Society of America*, Vol. 98, pp. 403-412, 1995.
- [12] ANSYS, "ANSYS Elements Reference," in ANSYS Elements Reference, vol. 11th Edition, ANSYS, Ed. Canonsburg, PA 15317: SAS IP, pp. Plane 13.
- [13] Inc. Eveready Battery Company, "Eveready No. A92," vol. 2002, Form NO. EBC - 1190A ed: Eveready Battery Company, Inc., 2002.
- [14] C. Theurer, L. Zhang, D. Kazmer, and R. Gao, "Threshold Energy Switching and its Application to Wireless Sensing in High Energy Manufacturing Processes," ASME International Mechanical Engineering Congress and Exhibition (IMECE), Symposium on Intelligent Sensors, New Orleans, LA, 2002.
- [15] L. Zhang, C. Theurer, R. Gao, and D. Kazmer, "Development of a Wireless Pressure Sensor for Remote Acoustic Transmission," *Transactions of the NAMRI/SME*, 2002.